Photonic crystal horizontally slotted nanobeam cavity for silicon-based nanolasers

Tsan-Wen Lu, Pin-Tso Lin, and Po-Tsung Lee*

Department of Photonics and Institute of Electro-Optical Engineering, National Chiao Tung University, Room 415 CPT Building, 1001 Ta-Hsueh Road, Hsinchu 300, Taiwan

**Corresponding author: potsung@mail.nctu.edu.tw*

Received October 28, 2011; revised December 15, 2011; accepted December 30, 2011; posted January 4, 2012 (Doc. ID 157205); published February 8, 2012

We theoretically propose and investigate a TM-polarized one-dimensional photonic crystal nanocavity with a horizontal SiO_2 slot on a suspended silicon nanobeam via the three-dimensional finite-element method. The ultrahigh quality factor and ultrasmall effective mode volume of 1.5×10^7 and 0.176 half-wavelength cubic of the horizontally SiO_2-slotted nanocavity show strong possibilities for realizing an erbium-doped SiO_2 nanolaser. This horizontal SiO_2 slot structure can be precisely formed via the sputtering process and further transformed into an air slot via selective wet etching for optical index and biomolecule sensing. © 2012 Optical Society of America

OCIS codes: 230.5298, 230.5750.

The silicon (Si)-based nanolaser source has long been regarded as the most important core on the blueprint for constructing complementary metal-oxide semiconductor (CMOS) processing compatible on-chip photonic integrated circuits (PICs) for all-optical information processing. To realize Si-based nanolasers, efficient optical emissions from Si-based materials [1] and nanocavity designs with low optical losses are essential. For the former, the erbium (Er)-doped SiO_2 with strong optical emissions near wavelength of 1.54 μm via excited electron transition from $^4I_{13/2}$ to $^4I_{15/2}$ states of the Er dopant [2] has been widely used in various active devices in optical communication systems. Although Er-doped SiO_2 microlasers via microtoroid [3] and microdisk [4] with total-internal-reflection (TIR) confinement have been demonstrated recently, the cavity sizes have to be sufficiently large (several tens of micrometers) to ensure adequately high quality (Q) factors for lasing due to the low index ($n_{SiO_2} \sim 1.45$) of SiO_2. Even utilizing photonic crystal (PhC) nanocavity [5,6] can efficiently confine photons in one-wavelength cubic volume, photonic bandgap (PBG) and TIR effects are weak owing to the low index of SiO_2. And the theoretical Q is limited to only 2.5×10^4 [7,8] and insufficient for lasing via the gain medium of Er-doped SiO_2 [4]. In this Letter, we propose and investigate a TM-polarized one-dimensional (1D) PhC SiO_2-slotted nanocavity with ultrahigh Q factor and extremely small mode volume (V_{eff}) on a suspended Si nanobeam (NB), which shows the strong possibilities for realizing an Er-doped SiO_2 nanolaser.

Our design starts from a 1D PhC nanocavity on a suspended Si NB shown in Fig. 1(a). The 1D PhCs are composed of air holes on the NB, where the TE/TM PBG effects exist simultaneously [9]. The mirror of the nanocavity is formed by 12-period gradually varied PhCs and a 10-period outer PhC mirror. The lattice constant (a_n, $n = 1 - 13$) of the gradually varied PhCs is linearly varied with a 5 nm increment under the fixed air-hole radius (r_n) over a_n (r_n/a_n) ratio of 0.32. The refractive index (n_{NB}) and width (w) of the Si NB are set as 3.48 and 340 nm, respectively. Via the three-dimensional (3D) finite-element method (FEM), we calculate the Q factors of the TM-polarized zeroth-order mode in nanocavities with different NB thickness t_{NB} from 300 to 1100 nm, as shown in Fig. 1(b). The Q factor increases with the t_{NB} and shows a saturated value as high as 9.7×10^6 when $t_{\text{NB}} = 900$ nm. The simulated mode profile for the E_z field in the x–y plane is shown in the inset of Fig. 1(b).

We then designed an Er-doped SiO_2 layer with thickness of t_{SiO_2} in the Si NB to form a horizontal SiO_2 slot structure. The Er-doped SiO_2 layer was embedded through the entire Si NB and served as the gain medium. And the PhCs (air holes) penetrate through this SiO_2-slotted Si NB vertically, as shown in Fig. 2(a). For the E_z field of the TM-polarized zeroth-order mode, the SiO_2 slot shows an index discontinuity in the z direction. Because the electric flux density has to satisfy the Maxwell equations, the E_z field will obey the relationship of $\varepsilon_{\text{Si}} E_{z\text{Si}} = \varepsilon_{SiO_2} E_{zSiO_2}$ [10], where ε_{Si}, ε_{SiO_2}, $E_{z\text{Si}}$, and E_{SiO_2} represent the dielectric constants and the E_z-field distributions of Si and SiO_2. Thus, the E_z field in the SiO_2 slot will show $\varepsilon_{\text{Si}}/\varepsilon_{SiO_2}$ times enhancement to that in Si and V_{eff} of the TM-polarized zeroth-order mode will also be greatly reduced.

With a fixed t_{NB} of 900 nm, the simulated Q factors and V_{eff} of the TM-polarized zeroth-order modes in 1D PhC

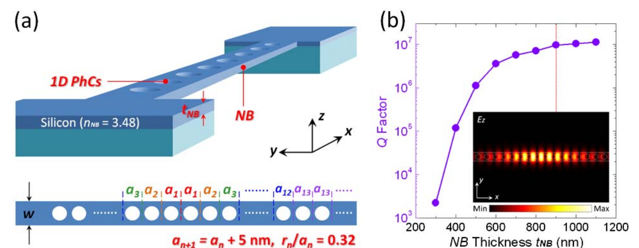

Fig. 1. (Color online) (a) Scheme and design of a 1D PhC nanocavity on a suspended Si NB. (b) Simulated Q factors of the TM-polarized zeroth-order modes in the 1D PhC NB nanocavities with different t_{NB} from 300 to 1100 nm. Inset, simulated mode profile for the E_z field in the x–y plane of the nanocavity with $t_{\text{NB}} = 900$ nm.

 © 2012 Optical Society of America

SiO_2-slotted NB nanocavities with different t_{SiO_2} are shown in Fig. 2(b). The Q factor increases to 1.5×10^7 when $t_{SiO_2} = 20$ nm, which is even higher than that of the nanocavity without the SiO_2 slot. This enhanced Q factor when t_{SiO_2} increases from 0 to 20 nm comes from the reduced effective index mismatching by the presence of the low-index SiO_2 slot with fine index tuning. However, once the t_{SiO_2} becomes larger than 20 nm, the effective index mismatching will increase, which significantly degrades the Q factor. The simulated mode profiles for the E_z field in the x–y, y–z, and x–z planes when $t_{SiO_2} = 20$ nm are shown in Fig. 2(c), where the E_z field is strongly enhanced inside the SiO_2 slot. Furthermore, the V_{eff} monotonically decreases with decreasing t_{SiO_2}, which can be understood by the $|E_z|^2$ distributions along the z axis of the nanocavities with different t_{SiO_2} shown in Fig. 2(d). When $t_{SiO_2} = 10$ nm, the V_{eff} and Q/V_{eff} are $0.176(\lambda/2n_{SiO_2})^3$ and $5.9 \times 10^7(\lambda/2n_{SiO_2})^{-3}$. The ultrahigh Q/V_{eff} is not only beneficial for realizing nanolasers, but it is also useful to the researches of quantum-electrodynamics (QED) and applications requiring strong light–matter interactions. In addition to the Er-doped SiO_2, we simulate the Er-doped SiN_x slot with the higher index of 2.0 as the gain material in our design. The simulated Q factors and V_{eff} of SiN_x-slotted nanocavities with different SiN_x thicknesses t_{SiN_x} and fixed t_{NB} of 900 nm are shown in Fig. 2(b). The Q factor shows an optimized value of 1.84×10^7 when $t_{SiN_x} = 80$ nm and the Q/V_{eff} reaches as high as $1.16 \times 10^7(\lambda/2n_{SiN_x})^{-3}$ when $t_{SiN_x} = 10$ nm. These values are both better than those of the reported 1D and 2D SiN_x PhC nanocavities [11,12].

There are several unique features and advantages in the presented horizontally slotted nanocavity design. First, for a 1D PhC nanocavity based on effective index matching, the horizontal slot formed on the entire NB can plays the role of index tuner to further optimize the Q factor, which means the V_{eff} can be greatly minimized while the Q factor remains high. Second, the most important advantage, the horizontal slot can be easily made via the sputtering process or chemical vapor deposition (CVD) with nanometer-scale precision, while the optimized electron beam lithography and dry etching processes in PhC vertically slotted nanocavities are not needed. In addition, compared with the traditional vertical slot formed by etching process, excellent uniformity and minimized surface roughness of the horizontal slot formed by sputtering process also greatly improve the losses at the interfaces of the slot and the Si. Third, the optical gain medium, the Er dopant, can be placed in the horizontal slot by cosputtering or the ion-implantation process during or after slot formation, which cannot be achieved in most reported PhC nanocavities with vertical slots. Moreover, via the slot, the radiative photon lifetime of the gain medium can be significantly extended [13]. Thus, with the enhanced mode properties and ease of insertion of the optical gain medium, utilizing our proposed horizontally slotted nanocavity to realize the Si-based nanolasers is possible. Furthermore, the presented nanocavity is also suitable for PhC quantum cascade lasers with TM polarization that lack a high Q cavity design before [14,15].

To evaluate the required minimum Q (Q_{lasing}) of the horizontally slotted nanocavities with different t_{SiO_2}/t_{SiN_x} for lasing, the gain condition of the Er dopant and the optical loss of the nanocavity are considered via the following equation [4]:

$$Q_{\mathrm{lasing}} > \frac{2\pi}{\lambda} n_{\mathrm{slot}} \frac{1}{\Gamma \sigma_\varepsilon N_{\mathrm{Er}}}. \quad (1)$$

The terms σ_ε and N_{Er} represent the emission cross section and concentration of the Er, which are set as 4×10^{-21} cm^2 and 1×10^{22} $\mathrm{ions/cm}^3$. The value of N_{Er} is chosen as the upper limit before clustering of the Er [4]. The mode overlap Γ factor with the Er-doped SiO_2/SiN_x slot is defined as the ratio of the $|E|^2$ field of the mode concentrating inside the slot. The simulated Q_{lasing} factors under different t_{SiO_2}/t_{SiN_x} are shown in Fig. 3(a), which strongly depend on the Γ factors also shown in Fig. 3(a). For t_{SiO_2} and t_{SiN_x} equal to 10 nm, the Γ factors are 0.193 and 0.077, respectively, while the Q_{lasing} factors reach their highest values of 7.6×10^3 and 2.64×10^4. Compared

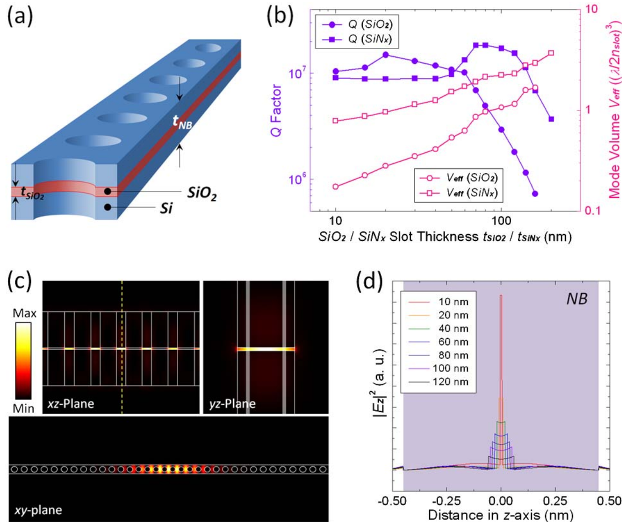

Fig. 2. (Color online) (a) Scheme of 1D PhC nanocavity on a horizontally SiO_2-slotted Si NB. (b) Simulated Q factors and V_{eff} of the TM-polarized zeroth-order modes in 1D PhC SiO_2/SiN_x-slotted nanocavities with $t_{SiO_2}/t_{SiN_x} = 10-160/200$ nm. (c) Simulated mode profiles for the E_z field in the x–z, y–z, and x–y planes when $t_{SiO_2} = 20$ nm. (d) Simulated $|E_z|^2$ distributions along the z axis [the dotted line in (c)] of the nanocavities with different t_{SiO_2}.

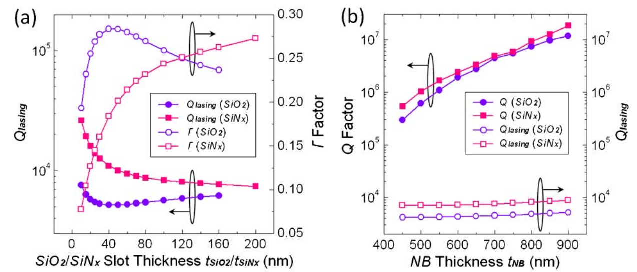

Fig. 3. (Color online) (a) Q_{lasing} and Γ factors of 1D PhC SiO_2/SiN_x-slotted NB nanocavities with different t_{SiO_2} and t_{SiN_x}. (b) Simulated Q and Q_{lasing} factors of 1D PhC SiO_2/SiN_x-slotted NB nanocavities with different t_{NB}, while the t_{SiO_2} and t_{SiN_x} are fixed at 40 and 80 nm, respectively.

with the simulated results in Fig. 2(b), the Q factors of the nanocavities with present t_{SiO_2}/t_{SiN_x} ranges are much higher (more than 2 orders at least) than the Q_{lasing} factors and show they are sufficient for lasing. Even taking the losses arisen from fabrication imperfections in a real situation [5,16] into consideration, the huge excess of the Q factors ensure the lasing capabilities of our design. In contrast, for the TE-polarized modes, the presented horizontally slotted nanocavity does not show a discontinuity in the index for their electric fields (E_x and E_y). Therefore, the electric fields will not tend to concentrate inside the SiO_2/SiN_x slots, which lead to very low Γ factors and over 1 order higher Q_{lasing} factors than those of the TM-polarized modes. Furthermore, to minimize the NB volume and simplify the sputtering process in fabrication, we also calculate the Q and Q_{lasing} factors of the nanocavities with different t_{NB} from 450 to 900 nm, as shown in Fig. 3(b). According to the Γ and Q factors, t_{SiO_2} and t_{SiN_x} are fixed at 40 and 80 nm, respectively. In Fig. 3(b), the Q factors decrease rapidly with the decreasing t_{NB} and are still 2 orders higher than the Q_{lasing} factors when $t_{NB} > 450$ nm for SiO_2/SiN_x-slotted nanocavities. These results show the lasing from the Er-doped SiO_2/SiN_x-slotted nanocavity can still be achieved under reasonable t_{NB}.

Based on our presented design, the air slots widely utilized in optical sensing [17–19] in recent years can be easily formed with different thicknesses t_{slot} by removing the SiO_2/SiN_x via proper selective chemical vapor wet etching [5]. To find the sensing capabilities, the environmental index is varied from 1.342 to 1.414. For the nanocavity with the horizontal air slot thickness t_{slot} of 80 nm, a high index sensitivity [defined as wavelength shift (nm) per refractive index unit (RIU) variation] of 280 nm/RIU and a small minimum detectable index variation at the level of 10^{-6} are obtained. In addition, owing to the enhanced electric field inside the air slot, the horizontally air-slotted nanocavity would also be very suitable for sensing biomolecules and can be applied for medical or biological label-free sensing applications via proper functionalization.

In summary, we propose a TM-polarized 1D PhC nanocavity with a low-index (SiO_2/SiN_x) horizontal slot on a suspended Si NB, where the slot can be easily prefabricated by sputtering or the CVD process with ultrafine control of thickness, uniformity, and surface roughness. Via 3D FEM simulations, the SiO_2 slot can greatly minimize the mode volume [$\sim 0.176(\lambda/2n_{SiO_2})^3$ when $t_{SiO_2} =$ 10 nm] and keep the Q very high ($\sim 1.5 \times 10^7$ when $t_{SiO_2} = 20$ nm) simultaneously, which are very beneficial for studying QED phenomenon and applications requiring strong light–matter interactions. Moreover, the ease of placing the gain medium (Er-doped SiO_2/SiN_x) inside the slot provides strong possibilities for realizing Er-doped SiO_2/SiN_x nanolasers for CMOS-processing-compatible PICs. By considering the gain conditions of the Er dopant in the SiO_2/SiN_x slots, the Q factors of nanocavities with presented slot thickness ranges are sufficient for lasing.

This work is supported by Taiwan's National Science Council (NSC) under contract nos. NSC-100-2221-E-009-109-MY3 and NSC-100-2120-M-009-005. The authors would like to acknowledge the help from the Center for Nano Science and Technology (CNST) of National Chiao Tung University (NCTU), Taiwan.

References

1. J. M. Shainline and J. Xu, Laser Photon. Rev. **1**, 1 (2007).
2. H. Ennen, J. Schneider, G. Pomrenke, and A. Axmann, Appl. Phys. Lett. **43**, 943 (1983).
3. A. Polman, B. Min, J. Kalkman, T. J. Kippenberg, and K. J. Vahala, Appl. Phys. Lett. **84**, 1037 (2004).
4. T. J. Kippenberg, J. Kalkman, A. Polman, and K. J. Vahala, Phys. Rev. A **74**, 051802 (2006).
5. P. B. Deotare, M. W. McCutcheon, I. W. Frank, M. Khan, and M. Lončar, Appl. Phys. Lett. **94**, 121106 (2009).
6. Y. Zhang, M. Khan, Y. Huang, J. H. Ryou, P. B. Deotare, R. Dupuis, and M. Lončar, Appl. Phys. Lett. **97**, 051104 (2010).
7. Y. Gong and J. Vučković, Appl. Phys. Lett. **96**, 031107 (2010).
8. Y. Gong, S. Ishikawa, S. L. Cheng, M. Gunji, Y. Nishi, and J. Vučković, Phys. Rev. B **81**, 235317 (2010).
9. Y. Zhang, M. W. McCutcheon, I. B. Burgess, and M. Lončar, Opt. Lett. **34**, 2694 (2009).
10. V. R. Almeida, Q. Xu, C. A. Barrios, and M. Lipson, Opt. Lett. **29**, 1209 (2004).
11. M. Khan, T. Babinec, M. W. McCutcheon, P. Deotare, and M. Lončar, Opt. Lett. **36**, 421 (2011).
12. M. Barth, J. Kouba, J. Stingl, B. Löchel, and O. Benson, Opt. Express **15**, 17231 (2007).
13. C. Creatore, L. C. Andreani, M. Miritello, R. Lo Savio, and F. Priolo, Appl. Phys. Lett. **94**, 103112 (2009).
14. M. Bahriz, V. Moreau, R. Colombelli, O. Crisafulli, and O. Painter, Opt. Express **15**, 5948 (2007).
15. Y. Chassagneux, R. Colombelli, W. Maineult, S. Barbieri, S. P. Khanna, E. H. Linfield, and A. G. Davies, Appl. Phys. Lett. **96**, 031104 (2010).
16. T. Asano, B. S. Song, and S. Noda, Opt. Express **14**, 1996 (2006).
17. A. Di Falco, L. O'Faolain, and T. F. Krauss, Appl. Phys. Lett. **94**, 063503 (2009).
18. J. Jágerská, H. Zhang, Z. Diao, N. Le Thomas, and R. Houdré, Opt. Lett. **35**, 2523 (2010).
19. S. Kita, S. Hachuda, S. Otsuka, T. Endo, Y. Imai, Y. Nishijima, H. Misawa, and T. Baba, Opt. Express **19**, 17683 (2011).